Biosensors and Bioelectronics 26 (2010) 1104–1108

Contents lists available at ScienceDirect

Biosensors and Bioelectronics

journal homepage: www.elsevier.com/locate/bios

Short communication

Noncovalently functionalized multi-wall carbon nanotubes in aqueous solution using the hydrophobin HFBI and their electroanalytical application

Xinsheng Wang[a], Huicai Wang[a], Yujian Huang[b], Zixia Zhao[c], Xia Qin[a], Yanyan Wang[a], Zhiying Miao[a], Qiang Chen[a,*], Mingqiang Qiao[b,**]

[a] The Key Laboratory of Bioactive Materials, Ministry of Education, College of Life Sciences, Nankai University, Weijin Road No. 94, Tianjin 300071, PR China
[b] The Key Laboratory of Molecular Microbiology and technology, College of Life Sciences, Nankai University, Tianjin 300071, PR China
[c] The Center for Applied Aquatic Genomics Chinese Academy of Fishery Sciences, Beijing 100141, PR China

ARTICLE INFO

Article history:
Received 19 April 2010
Received in revised form 22 July 2010
Accepted 12 August 2010
Available online 20 August 2010

Keywords:
Multi-wall carbon nanotubes
Hydrophobin
Nanocomposite materials
Electrochemistry
Biosensor

ABSTRACT

A novel noncovalent approach was developed for the functionalization of multi-wall carbon nanotubes (MWNTs) using the hydrophobin, HFBI. Owing to the amphipathic nature, HFBI can be adopted onto the surface of MWNTs to form HFBI–MWNTs nanocomposite with good dispersion in water. The HFBI–MWNTs nanocomposite was characterized by scanning electron microscopy (SEM), transmission electron microscopy (TEM) and water contact angle measurements (WCA). Furthermore, a glucose biosensor was developed based on HFBI–MWNTs by a one-step casting method. The resulting biosensor displayed high sensitivity, wider linear range, low detection limit, and fast response for glucose detection, which implicated that the HFBI–MWNTs nanocomposite film holds great promise in the design of electrochemical devices, such as sensors and biosensors.

1. Introduction

Due to their large surface area, unique structures, excellent electrical conductivity, ultra-strong mechanical properties and high stability, carbon nanotubes (CNTs) have been rapidly becoming electrode material (Peng et al., 2010). However, CNTs are commonly insoluble in all solvents and usually form tangled network structures containing various impurities (Chen et al., 1998; Wu et al., 2010). To overcome these limits, CNT surfaces are often tailored using either covalent (Balasubramanian and Burghard, 2005; Wu et al., 2007) or noncovalent modification (Chen et al., 2001; Hecht et al., 2006) strategies. Covalent surface modifications usually perturb the structures of nanotubes, and thus greatly change their desirable physical and chemical properties. Alternatively, efficient solubilization of CNTs has been demonstrated using the noncovalent adsorption of surfactants (Hu et al., 2007), polymers (Choi et al., 2010), and biomolecules such as DNA (Li et al., 2009), polysaccharides (Zhang et al., 2009a) and designed peptides (Salzmann et al., 2008; Witus et al., 2007). Recently, protein encapsulation of the CNTs was reported to be well dispersed in water (Hirano et al., 2009; Kurppa et al., 2007).

Hydrophobins are small proteins (~100 amino acids) that play various roles in fungal physiology related to surface phenomena, such as adhesion, formation of surface layers, and lowering of surface tension (van Wetter et al., 2000; Wösten et al., 1993; Wessels et al., 1991). As a remarkable property, hydrophobins have both hydrophobic and hydrophilic parts which make them easy to self-assemble at various interfaces to form polymeric amphipathic membranes and effect the reversal of the surfaces wettability. They are also among the most surface-active molecules known. Their activity is at least similar to that of traditional biosurfactants encompassing glycolipids, lipopeptides/lipoproteins, phospholipids, neutral lipids, substituted fatty acids, and lipopolysaccharides (Wösten and de Vocht, 2000). However, in contrast to these surfactants, surface activity depends on a conformational change of the molecules during assembly rather than on a diffusion-limited adsorption to the interface (van derVegt et al., 1996). Utilization of the properties of hydrophobins in applications such as coatings, emulsion stabilization, and separation technologies has been discussed (Hektor and Scholtmeijer, 2005). Recently, the ability of hydrophobins to improve the dispersibility of hydrophobic particles in water (Kurppa et al., 2007; Lumsdon et al., 2005) has been demonstrated. In addition, the protein presents numerous reactive groups such as hydroxyls, amines, thiols, and

* Corresponding author. Tel.: +86 22 23506173; fax: +86 22 23506122.
** Corresponding author. Tel.: +86 22 23503340; fax: +86 22 23503692.
E-mail addresses: qiangchen@nankai.edu.cn (Q. Chen), mingqiangqiao@yahoo.com.cn (M. Qiao).

0956-5663/$ – see front matter © 2010 Elsevier B.V. All rights reserved.
doi:10.1016/j.bios.2010.08.024

carboxylic acids which provide sites for further surface modification of the CNTs.

In the present paper we report a simple method for the solubilization of multi-wall carbon nanotubes (MWNTs) in water using a 7.5-kDa hydrophobin, HFBI. The HFBI-functionalized MWNTs (HFBI–MWNTs) was stable in water and able to form uniform MWNTs film at Pt electrode when dried. Furthermore, an amperometric glucose biosensor based on HFBI–MWNTs and glucose oxidase (GOD) has been developed to evaluate the performance of HFBI–MWNTs nanocomposite film in electrochemical applications. To the best of our knowledge, this is the first demonstration of an electrochemical biosensor based on the integration of GOD with carbon nanotubes functionalized by hydrophobin.

2. Experimental

2.1. Chemicals and reagents

MWNTs (10–20 nm diameter, 5–15 μm average length and >95% purity) were obtained from Shenzhen Nanotech Port Ltd. Co. (China). HFBI from *Trichoderma reesei* (p*I* 5.7, in 0.1 M NaCl ≥98% by agarose gel electrophoresis, lyophilized powder containing 30.9 wt.% HFBI) was isolated and purified as previously reported (Hou et al., 2008). GOD (EC 1.1.3.4, 235 units mg^{-1}, from *Aspergillus niger*), was purchased from Sigma. 4 mg mL^{-1} of GOD was prepared in 0.1 M phosphate buffer solution (PBS, pH 6.8). Glucose solutions were left overnight before use to allow equilibration of anomers. All other reagents were of analytical grade. All aqueous solutions were prepared with doubly distilled water.

2.2. Instrumentation

Electrochemical measurements were performed on a Potentiostat–Galvanostat (Model 283 with a software M270, EG&G Co.) A conventional three-electrode system comprising the modified platinum disk electrode as working electrode, a platinum wire (1 mm diameter) as counter electrode and an Ag/AgCl (saturated KCl) as reference electrode was employed for all electrochemical experiments in an electrochemical cell filled with 20 mL of 0.1 M PBS at room temperature. In steady-state amperometric experiment, the potential was set at +600 mV under gently magnetic stirring. Before all chronoamperometric experiments, the potential of each electrode was held at +600 mV, allowing the background current to decay to a steady-state value. The morphology of MWNTs was characterized by transmission electron microscopy (TEM, Tacnai T20, Philips) and scanning electron microscopy (SEM, QUANTA 200, FEI Co.). WCAs were measured by an optical contact angle meter (OCA20, Dataphysics Inc.). All experiments were performed at room temperature, ~25 °C.

2.3. Dispersion of MWNTs in HFBI solutions

The preparation of HFBI-functionalized water-soluble MWNTs was carried out as follows: 20 mg of pristine MWNTs was first dissolved in 10 mL 20 μg mL^{-1} HFBI aqueous solution under strong stirring, and then dispersed in ultrasonic bath for at least 30 min. The functionalized MWNTs were separated from the suspension by centrifugation (10,000 rpm, 20 min) for twice.

2.4. Fabrication of modified electrodes

Platinum disk electrodes (3 mm diameter) were polished before each experiment with chamois leather containing 0.05 μm alumina powders, rinsed thoroughly with doubly distilled water, ultrasonically cleaned in ethanol and doubly distilled water, and dried at room temperature.

The HFBI–MWNTs nanocomposite films were prepared by casting a 6 μL of as-prepared HFBI–MWNTs dispersion onto the Pt electrode and air-dried. Through the same method, the HFBI modified electrode was prepared with 20 μg mL^{-1} HFBI solution. For preparing the HFBI–MWNTs–GOD/Pt electrode, the mixture containing the same volume of HFBI–MWNTs dispersion and GOD solution was homogenized by the ultrasonic dispersion of 10 min; 6 μL of the solution was cast onto the surface of a Pt electrode and dried in air. The modified electrodes were put on a shelf with the electrode surface upward at 4 °C when not in use. Each electrode was dust-protected and kept at constant humidity conditions.

3. Results and discussion

3.1. Morphology

The HFBI–MWNTs suspension prepared by strong stirring and ultrasonication can be readily dispersed in water and stable for at least 45 days at room temperature, no phase separation with aggregation of nanotubes at the bottom of the vials while the MWNTs dispersed in water without adding HFBI were aggregated at the bottom of the vials within 30 min (Fig. S1).

The nanostructures of the HFBI–MWNTs were investigated by transmission electron microscopy (TEM). As shown in Fig. 1A, the surface of pristine MWNTs dispersed in water looked clear without any extra phase adhering to them. The HFBI–MWNTs nanocomposite (Fig. 1B) seemed a little wider than that of the pristine nanotubes, indicating that the protein wrapped around the MWNTs. In the high magnification image, a core-shell structure was clearly observed. The core with graphite sheets corresponded to the tubes and the shell layer attached tightly to the outer graphite sheet with a thickness of ~4–10 nm. Due to the surface-active and amphiphilic properties, HFBI has a high tendency to migrate to hydrophobic–hydrophilic interfaces and was able to encapsulate and dissolve hydrophobic molecules into aqueous media (Szilvay et al., 2007; Linder et al., 2005). Proteins may act as pseudo surfactants which adsorb onto the MWNTs through hydrophobic interactions, while their hydrophilic groups interact with water and this process eventually leads to complete debundling of MWNTs in protein solutions.

The surface morphology and microstructure of an indicator electrode greatly impacts its reactivity and performance. Scanning electron microscopy (SEM) was employed to gain insights into the surface morphology of HFBI–MWNTs modified electrodes, as shown in Fig. 1C. It is clear that a highly uniform HFBI–MWNTs film was formed on the surface without assembling into tangled ropes, which was in agreement with the TEM images observations (Fig. 1B), suggesting HFBI should be an excellent dispersant for carbon nanotube dispersion.

3.2. Water contact angles

Apart from the effective solubilization to MWNTs, characterization by WCA measurements revealed another merit of the protein improving the hydrophilicity of modified surface. It is known that the improvement in hydrophilicity enhances the biocompatibility of the nanostructure surface for the immobilization of proteins, thereby preserving their natural structure and bioactivity.

The hydrophilicity of the bare and HFBI–MWNTs modified platinum surface was assessed by determining the contact angle of water droplets. The reported WCA values are averages of three measurements made on different positions of the sample surface. The results showed that the WCA of platinum surface decreased from

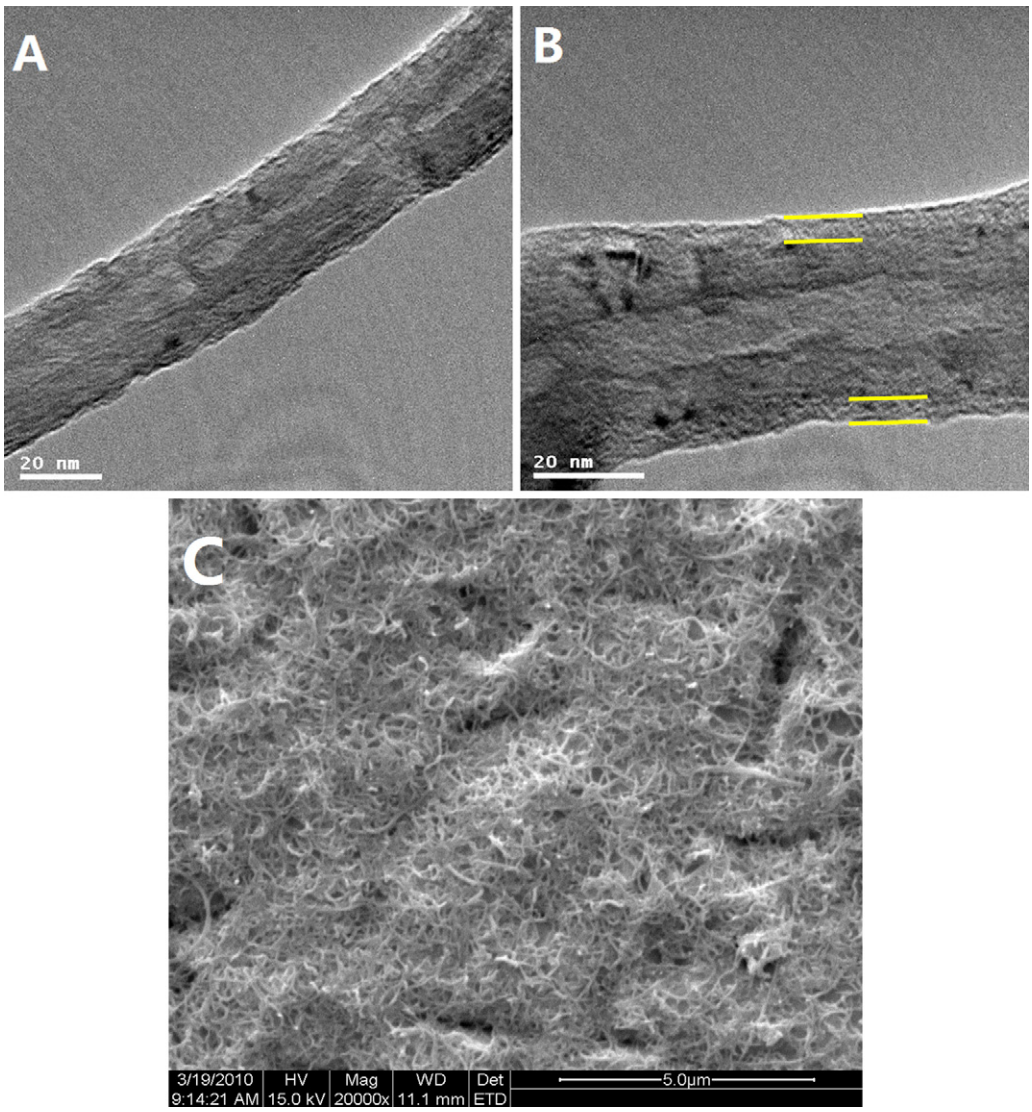

Fig. 1. TEM images of (A) pristine MWNTs and (B) HFBI–MWNTs; (C) SEM image of HFBI–MWNTs.

74.3° (±2.0°) to 13.2° (±2.0°) (n = 3) after modified by HFBI–MWNTs (Fig. S2), indicating the surface hydrophilicity was remarkably improved. We attempted to make an explanation to this change from two aspects. For the protein wrapped MWNTs, the hydrophobic part of HFBI faces to the wall of CNT, and the hydrophilic patch turns outside, inducing the reversal of the surface hydrophilicity. In addition, once coating, the non-conjugated HFBI will self-assemble on the platinum surface as most documents have reported (Corvis et al., 2005; Kisko et al., 2009). Besides, the WCA values of modified surfaces were not changed even after storing for several days.

3.3. Electrocatalytic activity of HFBI–MWNTs conjugates membrane

Cyclic voltammogram of the ferricyanide system is a convenient and valuable tool to monitor the characteristics of the surface of modified electrode. CVs of bare Pt, HFBI/Pt and HFBI–MWNTs/Pt conducted in 0.1 M KCl containing 20 mM $[Fe(CN)_6]^{3-}$ are shown in Fig. 2A. The peak current (i_p) of $[Fe(CN)_6]^{3-}$ increased and the peak-to-peak separation (ΔE_p) decreased in the order of HFBI/Pt, bare Pt and HFBI–MWNTs/Pt. A couple of well-defined peaks were observed for the HFBI–MWNTs/Pt at +290 mV and +142 mV. The peak-to-peak separations (ΔE_p) were 280.5 mV, 186 mV and 148 mV for HFBI/Pt, bare Pt electrode and HFBI–MWNTs/Pt, respectively, indicating the faster electron-transfer kinetics on HFBI–MWNTs modified electrode.

As shown in Fig. 2B, the i_p vs. square root of the scan rate was linear, which suggested a diffusion control in the process. The microscopic electroactive areas of the modified GCEs were obtained according to the Randles–Sevcik equation (Zhang et al., 2009b):

$$i_p = 2.69 \times 10^5 A D^{1/2} n^{3/2} \gamma^{1/2} C \quad (1)$$

where n is the number of electrons participating in the redox reaction and is equal to 1, A is the area of the electrode (cm^2), D is the diffusion coefficient of the molecule and is $(6.70 \pm 0.02) \times 10^{-6}\ cm^2\ s^{-1}$. C is the concentration of the probe molecule in the solution and is 20 mM, and γ is the scan rate ($V\ s^{-1}$). The active surface area for HFBI–MWNTs/Pt was $0.0916 \pm 0.0022\ cm^2$ compared to $0.0707\ cm^2$ for bare Pt electrode and $0.0481 \pm 0.0092\ cm^2$ for HFBI/Pt. Herein, the electron-blocking effect of HFBI was greatly improved after incorporating MWNTs and the HFBI–MWNTs modified Pt elecrode showed better electroactivity than both of the other two. The conclusion was further proved by CVs of bare Pt, HFBI/Pt and HFBI–MWNTs/Pt in 0.1 M PBS (pH6.8) (Fig. 2 inset).

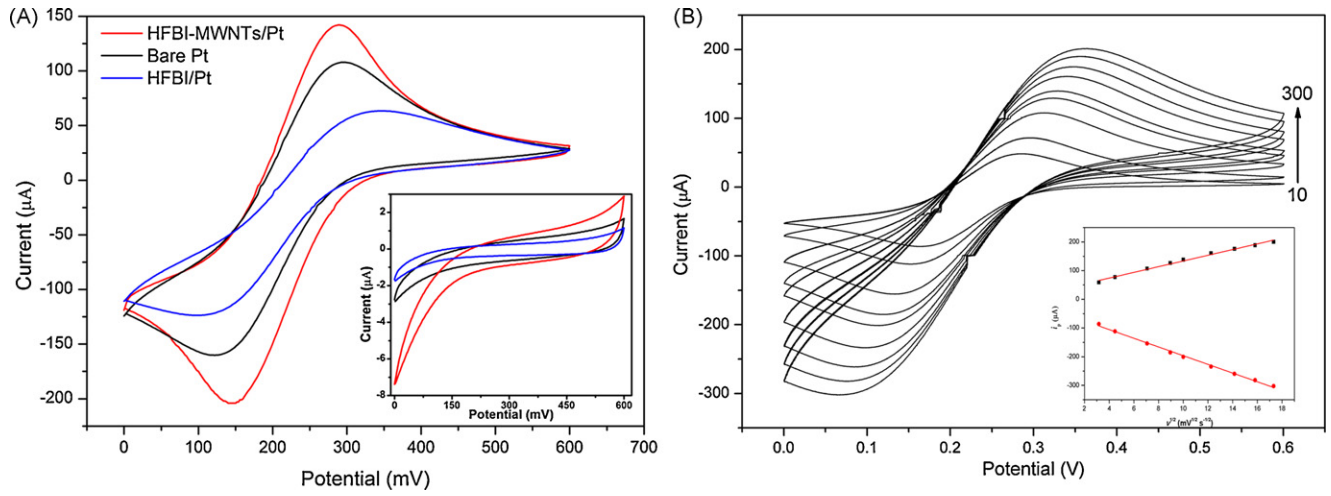

Fig. 2. (A) Cyclic voltammograms of bare Pt, HFBI/Pt and HFBI–MWNTs/Pt in 0.1 M KCl containing 20 mM $[Fe(CN)_6]^{3-}$ at 50 mV s^{-1}. Inset: cyclic voltammograms of the electrodes above in 0.1 M PBS (pH 6.8) (B) The HFBI–MWNTs modified electrodes at 10 mV s^{-1}, 20 mV s^{-1}, 50 mV s^{-1}, 80 mV s^{-1}, 100 mV s^{-1}, 150 mV s^{-1}, 200 mV s^{-1}, 250 mV s^{-1} and 300 mV s^{-1} (from inner to outer) in 0.1 M KCl containing 20 mM $[Fe(CN)_6]^{3-}$. Inset: plots of oxidation and reduction peak currents vs. $v^{1/2}$.

The stability and repeatability of the HFBI–MWNTs modified Pt electrode were tested in the ferricyanide system as described before. Only 1.18% decrease of oxidative currents from the 2nd to 20th cycle at the scan rate of 50 mV s^{-1} was observed (Fig.S3) and the RSD of peak current for the 20 cycles was 2.9%, indicating good stability and repeatability.

3.4. Chronoamperometric response

Since the modified electrode exhibits large active surface area and, fast electron-transfer kinetics and stable electrochemistry, it can be used as electron-transfer mediator to shuttle electrons between analytes and the electrode. GOD was selected as a model enzyme to evaluate the electrocatalytic ability of the HFBI–MWNTs modified Pt electrode. The glucose electrochemical biosensor is based on the amperometric detection of H_2O_2, which is generated during the course of the GOD-catalyzed oxidation of glucose in the presence of dissolved oxygen (Guiseppi-Elie et al., 2002). The typical current–time response of HFBI–MWNTs–GOD/Pt electrode for glucose detection at +600 mV was obtained in Fig. 3A. The biosensor reached 95% of the steady-state current within 8 s after the addition of glucose. After five independent repeating experiments, the steady-state calibration curve was fitted and shown in Fig. 3B. With the increasing glucose concentration, the amperometric response increased linearly in the range from 0.025 mM to 2.05 mM with a correlation coefficient of 0.998 (RSD varied from 3.2% to 4.7%, $n = 5$). The dynamic curve showed a sensitivity of 115.96 μA mM^{-1} cm^{-2} with a detection limit of 8.2 μM at the signal-to-noise ratio of 3.

The apparent Michaelis–Menten constant (K_m^{app}), which gives an indication of the enzyme–substrate kinetics for the glucose biosensor based on HFBI–MWNTs films, can be calculated from the Lineweaver–Burk equation (Kamin and Wilson, 1980):

$$\frac{1}{i_{ss}} = \left(\frac{K_m^{app}}{i_{max}}\right)\left(\frac{1}{C}\right) + \left(\frac{1}{i_{max}}\right) \quad (2)$$

where i_{ss} is the steady-state response current when substrates are added, i_{max} is the maximum current measured in saturated substrate conditions, and C represents the bulk concentration of the substrate. The K_m^{app} determined in the present studies (Fig. 3B, inset) was calculated to be 2.45 mM. The resulting biosensor displayed better performance than our group's previous investigation (Zhao et al., 2007), which constructed only used HFBI. The latter biosensor showed detection limits of 90 μM, linear range from 0.5 mM to 20 mM, sensitivity of 4.214 μA mM^{-1} cm^{-2} and K_m^{app} of 16.8 mM. Although additional calibration tests are required before further fabrication processes, this system is highly promising for the future development of glucose sensing.

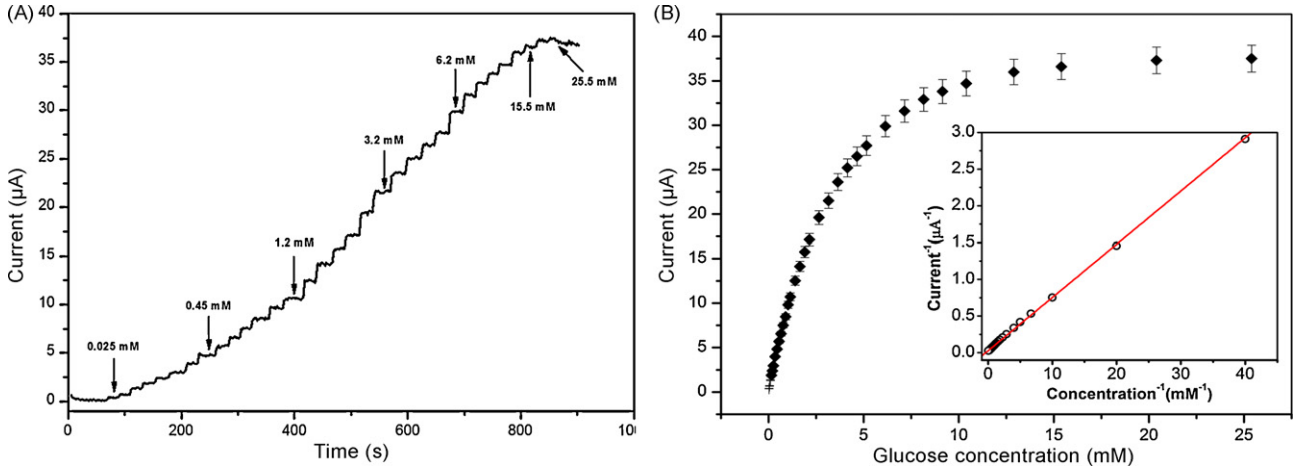

Fig. 3. (A) Typical amperometric response of the biosensor to successive addition of glucose into stirring PBS (pH 6.8) at +600 mV. (B) Steady-state calibration curve of the HFBI–MWNTs films modified Pt electrodes. Inset: Lineweaver–Burk plot of $1/i_{ss}$ vs. $1/C$. Error bars = ±standard deviation and $n = 5$.

The influences of ascorbic acid, uric acid and acetaminophen on the glucose response were minimized due to the optimum permeability of hydrophobin film (Zhao et al., 2007). In addition, this sensor has good stability (remains 83% of its initial response after being kept for one month) and reproducibility (parallel detection for five times with a RSD of 4.3%). It is notable the maximum current response did not appear right after the enzyme modification of electrode, but presented itself four days after the modification. The possible reason is related to protein rearrangement on the electrode surface and bioactivity recovery of enzyme (Zhao et al., 2007).

4. Conclusion

In summary, the hydrophobin HFBI demonstrates an efficient ability to be a solubilizing agent for MWNTs. The resulting HFBI–MWNTs nanocomposite film with both merits of HFBI and MWNTs exhibited high hydrophilicity, fast electron-transfer kinetics and excellent electrocatalytic activity. The glucose biosensor based on HFBI–MWNTs displayed high sensitivity, low detection limit, and fast response for glucose detection. The novel HFBI–MWNTs film can be easily applied to other types of substrate electrodes and surfaces and this will further broaden the electroanalytical applications.

Acknowledgements

The financial supports from National Natural Science Foundation of China (Grant nos. 30772746, 30870665 and 30900325), and Natural Science Foundation of Tianjin (Grant no. 08JCZDJC20600) are well acknowledged.

Appendix A. Supplementary data

Supplementary data associated with this article can be found, in the online version, at doi:10.1016/j.bios.2010.08.024.

References

Balasubramanian, K., Burghard, M., 2005. Small 1 (2), 180–192.
Chen, J., Hamon, M.A., Hu, H., Chen, Y.S., Rao, A.M., Eklund, P.C., Haddon, R.C., 1998. Science 282 (5386), 95–98.
Chen, R.J., Zhang, Y.G., Wang, D.W., Dai, H.J., 2001. J. Am. Chem. Soc. 123 (16), 3838–3839.
Choi, E.Y., Han, T.H., Hong, J.H., Kim, J.E., Lee, S.H., Kim, H.W., Kim, S.O., 2010. J. Mater. Chem. 20 (10), 1907–1912.
Corvis, Y., Walcarius, A., Rink, R., Mrabet, N.T., Rogalska, E., 2005. Anal. Chem. 77 (6), 1622–1630.
Guiseppi-Elie, A., Lei, C.H., Baughman, R.H., 2002. Nanotechnology 13 (5), 559–564.
Hecht, D.S., Ramirez, R.J.A., Briman, M., Artukovic, E., Chichak, K.S., Stoddart, J.F., Gruner, G., 2006. Nano Lett. 6 (9), 2031–2036.
Hektor, H.J., Scholtmeijer, K., 2005. Curr. Opin. Biotechnol. 16 (4), 434–439.
Hirano, A., Maeda, Y., Akasaka, T., Shiraki, K., 2009. Chem. Eur. J. 15 (38), 9905–9910.
Hou, S., Yang, K., Qin, M., Feng, X.Z., Guan, L., Yang, Y.L., Wang, C., 2008. Biosens. Bioelectron. 24 (4), 912–916.
Hu, C.G., Yang, C.H., Hu, S.S., 2007. Electrochem. Commun. 9 (1), 128–134.
Kamin, R.A., Wilson, G.S., 1980. Anal. Chem. 52, 1198–1205.
Kisko, K., Szilvay, G.R., Vuorimaa, E., Lemmetyinen, H., Linder, M.B., Torkkeli, M., Serimaa, R., 2009. Langmuir 25 (3), 1612–1619.
Kurppa, K., Jiang, H., Szilvay, G.R., Nasibulin, A.G., Kauppinen, E.L., Linder, M.B., 2007. Angew. Chem. Int. Ed. 46 (34), 6446–6449.
Li, Z.Z., Wu, Z.Y., Li, K., 2009. Anal. Biochem. 387 (2), 267–270.
Linder, M.B., Szilvay, G.R., Nakari-Setala, T., Penttila, M.E., 2005. FEMS Microbiol. Rev. 29 (5), 877–896.
Lumsdon, S.O., Green, J., Stieglitz, B., 2005. Colloid Surf. B: Biointerfaces 44 (4), 172–178.
Peng, L., You, S.J., Wang, J.Y., 2010. Biosens. Bioelectron. 25 (5), 1248–1251.
Salzmann, C.G., Lee, G.K.C., Ward, M.A.H., Chu, B.T.T., Green, M.L.H., 2008. J. Mater. Chem. 18 (17), 1977–1983.
Szilvay, G.R., Paananen, A., Laurikainen, K., Vuorimaa, E., Lemmetyinen, H., Peltonen, J., Linder, M.B., 2007. Biochemistry 46 (9), 2345–2354.
van derVegt, W., van derMei, H.C., Wösten, H.A.B., Wessels, J.G.H., Busscher, H.J., 1996. Biophys. Chem. 57 (2–3), 253–260.
van Wetter, M.A., Wösten, H.A.B., Wessels, J.G.H., 2000. Mol. Microbiol. 36 (1), 201–210.
Wösten, H.A.B., de Vocht, M.L., 2000. Bba-Rev Biomembranes 1469 (2), 79–86.
Wösten, H., De Vries, O., Wessels, J., 1993. Plant Cell 5 (11), 1567–1574.
Wessels, J., De Vries, O., Asgeirsdottir, S.A., Schuren, F., 1991. Plant Cell 3 (8), 793–799.
Witus, L.S., Rocha, J.D.R., Yuwono, V.M., Paramonov, S.E., Weisman, R.B., Hartgerink, J.D., 2007. J. Mater. Chem. 17 (19), 1909–1915.
Wu, B.Y., Hou, S.H., Yin, F., Zhao, Z.X., Wang, Y.Y., Wang, X.S., Chen, Q., 2007. Biosens. Bioelectron. 22 (12), 2854–2860.
Wu, H.C., Chang, X.L., Liu, L., Zhao, F., Zhao, Y.L., 2010. J. Mater. Chem. 20 (6), 1036–1052.
Zhang, X.K., Meng, L.J., Lu, Q.H., 2009a. Acs Nano 3 (10), 3200–3206.
Zhang, W., Yang, T., Zhuang, X.M., Guo, Z.Y., Jiao, K., 2009b. Biosens. Bioelectron. 24 (8), 2417–2422.
Zhao, Z.X., Qiao, M.Q., Yin, F., Shao, B., Wu, B.Y., Wang, Y.Y., Wang, X.S., Qin, X., Li, S., Yu, L., Chen, Q., 2007. Biosens. Bioelectron. 22 (12), 3021–3027.